Journal of Thermal Analysis, Vol. 38 (1992) 1921-1937

HEAT CAPACITY AND TRANSITION PHENOMENA OF STRUCTURE I AND II TRIMETHYLENE OXIDE CLATHRATE HYDRATES*

N. Kuratomi, O. Yamamuro, T. Matsuo and H. Suga

DEPARTMENT OF CHEMISTRY AND MICROCALORIMETRY RESEARCH CENTER, FACULTY OF SCIENCE, OSAKA UNIVERSITY, TOYONAKA, OSAKA 560, JAPAN

(Received 2 December 1991; accepted 20 January 1992)

Heat capacities of structure I and II trimethylene oxide (TMO) clathrate hydrates doped with small amount of potassium hydroxide (x= 1.8×10^{-4} to water) were measured by an adiabatic calorimeter in the temperature range 11–300 K. In the str. I hydrate (TMO·7.67H_2O), a glass transition and a higher order phase transition were observed at 60 K and 107.9 K, respectively. The glass transition was considered to be due to the freezing of the reorientation of the host water molecules, which occurred around 85 K in the pure sample and was lowered owing to the acceleration effect of KOH. The relaxation time of the water reorientation and its distribution were estimated and compared with those of other clathrate hydrates. The phase transition was due to the orientational ordering of the guest TMO molecules accommodated in the cages formed by water molecules. The transition was of the higher order and the transition entropy was 1.88 $J\cdot K^{-1}(TMO\text{-}mol)^{-1}$, which indicated that at least 75% of orientational disorder was remaining in the low temperature phase. In the str. II hydrates (TMO·17H_2O), only one first-order phase transition appeared at 34.5 K. This transition was considered to be related to the orientational ordering of the water molecules as in the case of the KOH-doped acetone and tetrahydrofuran (THF) hydrates. The transition entropy was 2.36 $JK^{-1}(H_2O\text{-}mol)^{-1}$, which is similar to those observed in the acetone and THF hydrates. The relations of the transition temperature and entropy to the guest properties (size and dipole moment) were discussed.

Keywords: adiabatic calorimeter, heat capacities, trimethylene oxide clathrate hydrates

* Contribution No 57 from the Microcalorimetry Research Center

John Wiley & Sons, Limited, Chichester
Akadémiai Kiadó, Budapest

Introduction

Clathrate hydrates [1–5] are well-known inclusion compounds which occur in nature. The host lattice is constructed by water molecules, forming a three-dimensional hydrogen bond network like various ice polymorphs. The guest molecules are accommodated with van der Waals interaction in the well-defined cages of the host lattice. More than 100 guest molecules have been known to be enclathrated so far in six types of host lattices depending on their sizes and shapes: most of them are enclathrated in structure I and II clathrate cages. The unit cell of the str. I host lattice is composed of 2 pentagonal dodecahedral and 6 tetrakaidecahedral cages formed by 46 water molecules, while that of str. II host lattice is composed of 16 pentagonal dodecahedral and 8 hexakaidecahedral cages formed by 136 water molecules.

One of the most interesting subjects in the clathrate hydrate research is the orientational disorder of both guest and host molecules. Orientational disorder in solids is usually removed through a phase transition at low temperature. In every clathrate hydrate, however, the orientational disorder of the water molecules is frozen-in before the crystal reaches its hypothetical ordering transition on cooling. Actually, a glass transition due to the freezing out of the water reorientational motion was observed by calorimetry in str. I ethylene oxide (EO) hydrate (80 K) [6], str. I and II trimethylene oxide (TMO) hydrates (90 K) [7], str. II tetrahydrofuran (THF) hydrate (85 K) [8], and str. II acetone hydrate (90 K) [9]. This behaviour of the water molecules is essentially the same as that of hexagonal [10] and cubic [11] ices. The ordering transition of the guest molecules has never been observed except for one special case. It is str. I TMO hydrate [7, 12], in which an ordering transition takes place at 107 K. The absence of the guest ordering in other hydrates is supposed to be due to the guest-host interaction overcoming the guest-guest one [13]. This means that a preferred direction of the guest molecule in each cage cannot be fixed owing to locally fluctuating electric field induced by the cage-forming water dipoles which are disordered in orientation.

In our recent heat capacity studies, a phase transition was found in str. II THF [14] and str. II acetone [15] hydrates doped with small amount of potassium hydroxide ($x = 1.8 \cdot 10^{-4}$ to water). The subsequent dielectric measurement of THF hydrate [16] showed that the orientational motion of water molecules was accelerated drastically by doping of KOH and both water and guest molecules are ordered concurrently at the transition. In KOH-doped str. II argon hydrate, however, no phase transition was induced [17]. A glass transition due to the freezing of water molecules was observed at 55 K. The acceleration effect of KOH on the water reorientation was first found in hexagonal ice [18, 19]; a phase transition due to the ordering of water orientation was induced at 72 K. The mechanism of the acceleration has not been clarified completely but it is believed that an ionic

L defect produced by substituting H_2O molecule by OH^- ion plays an important role.

In the present study, we measured the heat capacities of str. I and str. II TMO hydrates doped with KOH. TMO is an interesting guest molecule which can be enclathrated both in str. I and str. II host lattices. TMO molecules are accommodated only in tetrakaidecahedral cages in the str. I hydrate and only in hexakaidecahedral cages in the str. II hydrate. The corresponding compositions for the hydrates for the full occupation of the guest molecules are TMO·7(2/3)H_2O and TMO·17H_2O, respectively. Another interesting aspect of TMO is that the str. I hydrate is only one clathrate hydrate which exhibits a guest ordering transition as described above.

The first purpose of the present study is to clarify the effect of guest molecules on the ordering transition of str. II clathrate hydrates. The van der Waals diameter and dipole moment of the guest molecules whose KOH-doped hydrates have been measured so far and those of TMO molecule are as follows:

Guest	d_{vdW} / pm	μ / Debye
Ar	380	0
THF	590	1.63
acetone	630	2.88
TMO	550	1.93

TMO molecule has smaller size than those of THF and acetone and medium dipole moment between THF and acetone. The phase transition of the str. II TMO hydrate, if any, would provide important information to understand the mechanism of the ordering transition of str. II clathrate hydrates. The second purpose is to determine the precise thermodynamic quantities associated with the guest ordering transition of the str. I hydrate. It has been very difficult to form pure str. I TMO hydrate without any coexistence of str. II hydrate and TMO. It is hopeful to obtain an ideal composition of the str. I TMO hydrate in this study. The formation of the KOH-doped acetone hydrate is known to be much easier than that of the pure one [9, 15]. The third purpose of this study is to investigate the ordering, phenomenon of water orientation in the situation that the orientation of the guest molecules is already ordered. The str. I TMO hydrate is only one system with which this subject can be investigated.

Experimental

Samples

TMO (Tokyo Kasei Kogyo Co., Ltd.) was purified by fractional distillation with a rectifier having more than 80 theoretical plates (Shibata Kagaku Kikai Co., Ltd.). No trace of impurity was observed in the analysis with a gas chromatography (Perkin–Elmer F21). Water was also purified by distillation followed by deionization. Conductance of the purified water was about 60 $nScm^{-1}$.

The sample solutions of str. I and II hydrates were prepared gravimetrically as follows. First, KOH aqueous solution of 0.01 $mol \cdot dm^{-3}$, corresponding to mole fraction of $1.8 \cdot 10^{-4}$, was prepared by mixing a commercial KOH aqueous solution of 0.1 $mol \cdot dm^{-3}$ (Wako Pure Chemical Ind., Ltd.) and the purified water. This concentration was the same as the samples of the other KOH-doped hydrates studied before. After a careful degassing, the solution was charged into the calorimeter cell by an injector under helium atmosphere. The purified TMO was then introduced into the cell by vacuum distillation through a copper tube connected to the cell. Finally, a small amount of helium gas for the aids of good thermal contact between the cell and the sample was introduced into the dead space of the cell, and the copper tube was pinched off with soldering. For both sample solutions, the amounts of TMO, KOH-water, and helium gas and the resultant compositions are summarized below:

	str. I hydrate	str. II hydrate
TMO	$8.0110 \cdot 10^{-2}$ mol	$4.1741 \cdot 10^{-2}$ mol
KOH – water	$6.1385 \cdot 10^{-1}$ mol	$7.0913 \cdot 10^{-1}$ mol
helium gas	$1.8 \cdot 10^{-4}$ mol	$2.4 \cdot 10^{-4}$ mol
composition	$TMO \cdot 7.663H_2O$	$TMO \cdot 16.99H_2O$

Calorimeter

The sample cell used here was the same as that used in the study of the acetone and THF hydrates. The mass and inner volume of the cell were 34.850 g and 20.87 cm^3, respectively. The temperature was measured with Rh-Fe resistance thermometer (27 Ω at 273 K), which has been calibrated based on EPT-76 below 30 K and IPTS – 68 above 30 K.

A calorimeter with a built-in refrigerator [20] was used in this study. Low temperature down to 20 K was available without any coolant other than liquid nitrogen. This calorimeter was very useful for annealing experiment of the sample at temperatures below 77 K for a long time as performed in this study.

Heat capacity measurement was carried out in the temperature range 11–300 K for both samples: temperature below 20 K was attained by pumping liquid hydrogen produced in the coolant tank of the cryostat. The precision of the heat capacity measurement was about 1% below 20 K, 0.3% between 20 and 30 K, and 0.1% above 30 K.

Formation of the hydrates

TMO-H_2O binary system exhibits an incongruent type phase diagram possessing two peritectic points corresponding to str. I and str. II clathrate hydrates [21]. The stoichiometric composition and incongruent melting temperature of the str. I and str. II hydrates are TMO·7.67H_2O (253 K) and TMO·17H_2O (264 K), respectively. The temperature of the eutectic melting of TMO and TMO·7.67H_2O is 173.5 K.

The hydrate crystal was formed through the reaction of str. II hydrate crystal and TMO solution in the case of str. I hydrate, and through the reaction of ice and TMO solution in the case of str. II hydrate. These reactions advance very slowly because they occur at the interface between the crystal and the solution, being interfered with the formed hydrate crystal. In this study, the hydrate crystals were obtained by annealing the sample successively at several temperatures below each peritectic point. The annealing temperatures and times are as follows:

str. I hydrate	str. II hydrate
249 K (23 h)	263 K (67 h)
245 K (62 h)	260 K (68 h)
240 K (858 h)	255 K (90 h)

Before each change of the annealing temperature, the sample was cooled down to the temperature below the eutectic point (173.5 K) and then heated slowly up to the next annealing temperature. This manner of annealing may be effective to produce fresh reaction interface and new nucleus of the hydrate crystal. The extent of the hydrate formation was checked by measuring the enthalpy of the eutectic melting. At the final stage of the annealing, no trace of the unreacted solution was found for the str. II hydrate and about 1% of TMO was found for the str. I hydrate. This is the first occasion that a large amount of almost pure str. I TMO hydrate was obtained. The present successful formations of the hydrates are probably caused by KOH and the manner of the annealing as in the case of acetone hydrates [15].

The correction for the small contribution of heat capacity due to the unreacted part of the sample was performed carefully. This correction is very complicated

and the full details will be described in a separate paper [22]. Thus, all the thermodynamic quantities given below are reduced to the values for their stoichiometric compositions.

Results and discussion

Heat capacity of str. I hydrate

Figure 1 shows the heat capacities of the TMO str. I and str. II hydrates in the temperature range 0–150 K. The data above this range and all the numerical values will be presented in the next paper [22]. There are two heat capacity anomalies in the str. I hydrate; one is a peak at 118 K and the other is a jump around 60 K. Only one heat capacity peak at 35 K was observed in the str. II hydrate. It is interesting that a reversal in magnitude of the heat capacities of the str. I and str. II hydrate occurred at 50 K. In the following sections, these anomalies will be analyzed and discussed along with the comparison with the data of other clathrate hydrates studied so far.

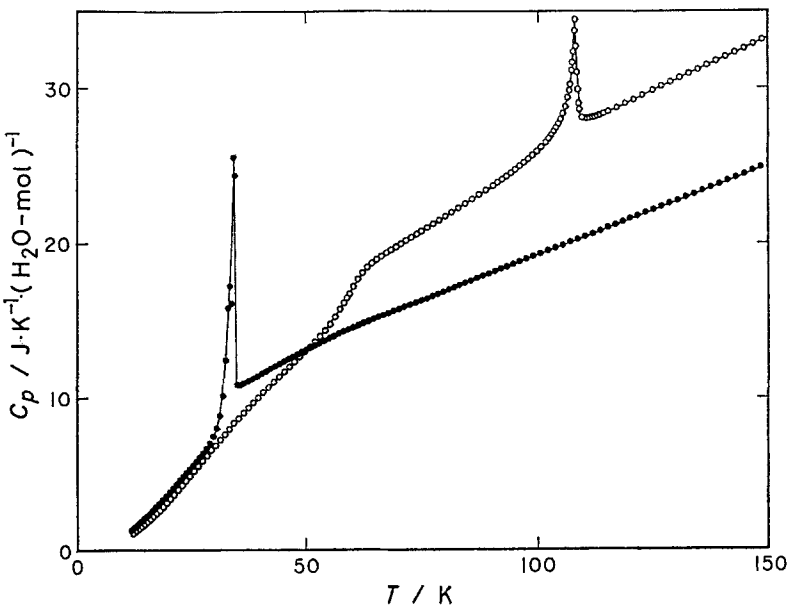

Fig. 1 Heat capacities of TMO·7.67H_2O (O) and TMO·17H_2O (•) doped with KOH (x = $1.8 \cdot 10^{-4}$)

Phase transition of str. I hydrate

Figure 2 shows the heat capacity peak observed in the str. I hydrate around 110 K. The transition was of a λ–type higher order. Even at the top of the heat capacity peak, shown in the magnified scale in the inset, thermal equilibrium after each energy input was attained immediately as in the temperature range free from the transition. The transition temperature was 107.91±0.02 K, which agreed with the transition temperature (107 K) reported by the previous heat capacity measurement [7]. Vibrational heat capacity around this region (baseline) was determined by fitting the experimental heat capacities below 80 K and above 135 K to a fifth-order power polynomial function. The determined baseline was shown as the curve in Fig. 2. The excess heat capacity due to the transition was calculated by subtracting this baseline from the total heat capacity and the transition entropy was then calculated by integrating the excess heat capacity divided by temperature. The temperature dependence of the transition entropy was given in Fig. 3 and its saturated value was 0.245 $J \cdot K^{-1}(H_2O\text{-mol})^{-1}$, corresponding to 1.88 $J \cdot K^{-1}(TMO\text{-mol})^{-1}$ (=R ln 1.25). This value is about 30% larger than the transition entropy obtained by Handa [7] (1.3 $J \cdot K^{-1}(TMO\text{-mol})^{-1}$ though his sample contained a small amount of the str. II hydrate as an impurity.

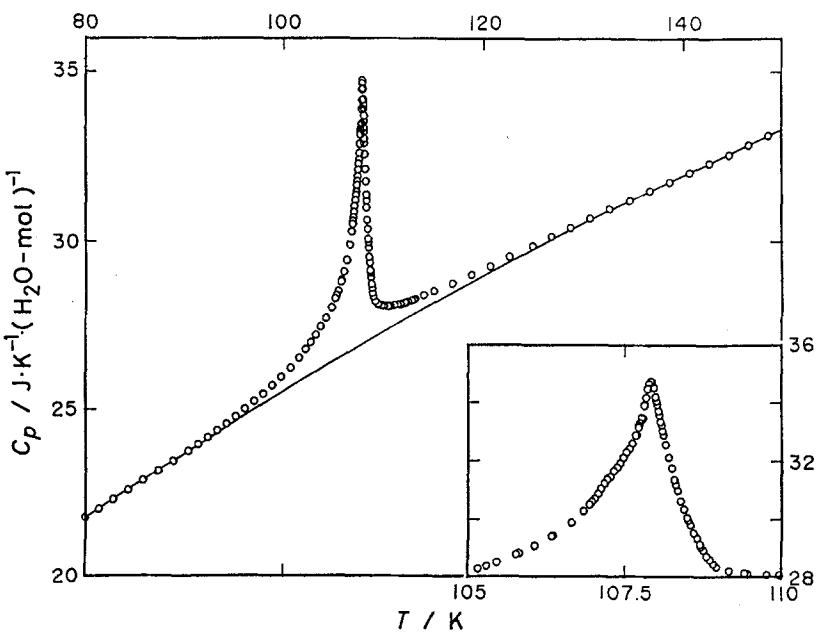

Fig. 2 Heat capacity of TMO·7.67H_2O (KOH: x = 1.8·10^{-4}) around the higher order transition

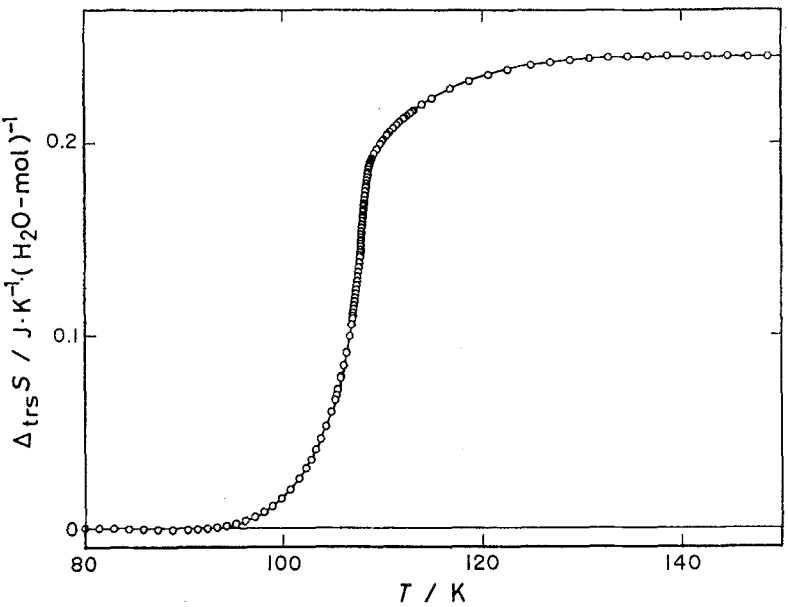

Fig. 3 Transition entropy of TMO·7.67H_2O (KOH: $x = 1.8 \cdot 10^{-4}$)

From the dielectric and NMR experiments [12], it is believed that this phase transition is related to the orientational ordering of the TMO molecules. In the str. I hydrate of ethylene oxide (EO) which has molecular structure similar to TMO, it is known by neutron diffraction [23] that an oxygen atom of EO molecule points to the center of the two hexagons of the tetrakaidecahedral cage. If the TMO molecule behaves like the EO molecule in the tetrakai-decahedral cage, the entropy of the ordering transition is expected to be 5.76 J·K^{-1}(TMO-mol)$^{-1}$(= R ln 2). The present experimental value is 32% of this, indicating that a major part of the disorder (75% from the simple calculation) persists in the low temperature phase. This result is consistent with the dielectric and NMR data [12], in which dielectric dispersion was still observed and a second moment of the NMR spectrum was smaller than the rigid-lattice value in the low temperature phase.

Glass transition of str. I hydrate

Figure 4 shows the spontaneous temperature drift rates observed during equilibration periods at 10 min after each energy input of the heat capacity measurement. In the sample cooled continuously at the rate of 0.5 K·min^{-1} (open circles), which corresponds to the data shown in Fig. 1, exothermic followed by endother-

mic temperature drifts appeared in the temperature range 40–65 K. On the other hand in the sample annealed at 52 K for 30 h, only endothermic drifts appeared starting from the annealing temperature. This type of temperature drift, which depends strongly on the thermal history of the sample, is one of the characteristic features of the glass transition [24]. The exothermic and endothermic drifts are due to the relaxation of the configurational enthalpy which is related to the molecular motion frozen out at the glass transition.

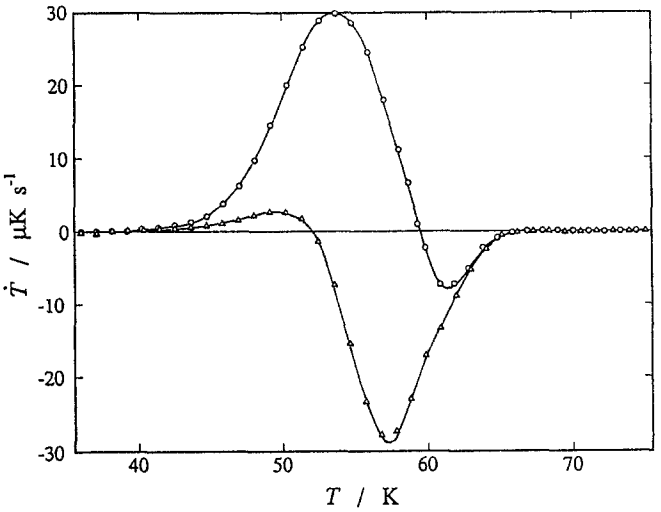

Fig. 4 Spontaneous temperature drift rate around the glass transition of TMO·7.67H_2O (KOH: $x = 1.8 \cdot 10^{-4}$). O : cooled continuously, Δ: annealed at 52 K for 30 h

In the pure (not doped with KOH) sample, a glass transition was observed around 90 K [7], at which no heat capacity anomaly was observed in the present sample. This indicates that the present glass transition is the one moved from 90 K by doping of KOH and is due to a freezing of the water reorientational motion. If the acceleration effect of KOH on the water motion is more significant, an ordering transition of the water orientation would appear below 60 K as in the case of THF and acetone str. II hydrates [14, 15]. The present situation is the same as that of the KOH-doped argon clathrate hydrate [17].

Figure 5 shows the diagram of the configurational enthalpy plotted against temperature around the glass transition. The step-like line represents the enthalpy path followed by the relaxing sample during the actual heat capacity mea-surement for the continuously cooled sample. The horizontal segment represents the temperature increase caused by each energy input and the vertical one the exothermic enthalpy relaxation observed during each equilibration period. The relaxation that might occur during each heating period is corrected for by ex-

trapolating the spontaneous temperature drift, so that the calculated heat capacity corresponds to the isoconfigurational heat capacity. The part of relaxation occurring during the heating is included in the vertical segment. The curve smoothly rising up to the right gives the hypothetical equilibrium enthalpy that would be realized in an ideal equilibrium experiment.

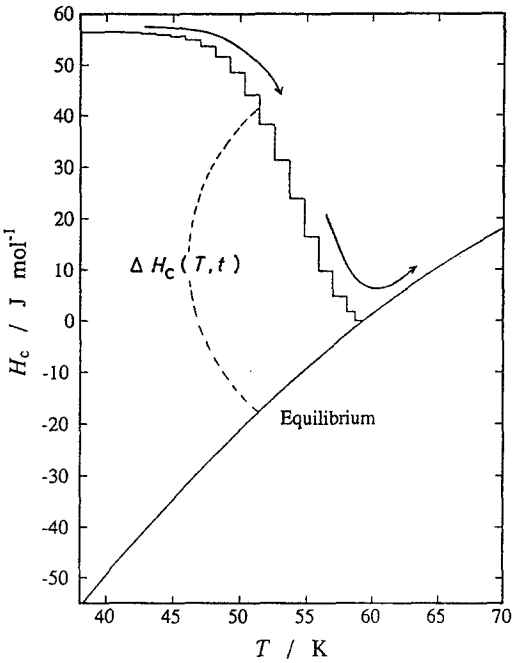

Fig. 5 Configurational enthalpy path followed by the sample during the heat capacity measurement around the glass transition of TMO·7.67H_2O (KOH: $x = 1.8 \cdot 10^{-4}$) (see text for details)

In most of the glassy crystals [25], the relaxation time $\tau(T)$ related to the glass transition can be calculated by use of the equation

$$\frac{d\,\Delta H_c(T,t)}{dt} = -\frac{\Delta H_c(T,t)}{\tau(T)} \quad (1)$$

Here, $\Delta H_c(T, t)$ and $d\Delta H_c(T, t)/dt$ are the enthalpy departure from the equilibrium state and its relaxation rate at temperature T and time t, respectively, both being estimated experimentally as described elsewhere [8]. This equation asserts an exponential enthalpy relaxation with a single time constant τ. Even in the case of the relaxation times with distribution, however, this equation is practically valid for the effective (averaged) relaxation time if the distribution is rather sharp and not modified much during the relaxation process [6]. Using the exo-thermic data of

the continuously cooled sample, the effective relaxation times of the TMO str. I hydrate were calculated at several temperatures 5–15 K lower than T_g where the conditions described above were supposed to be valid.

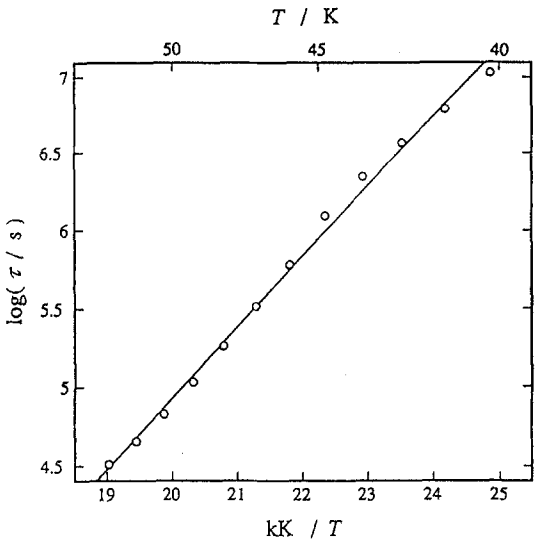

Fig. 6 Arrhenius plot of the relaxation time related to the glass transition of TMO·7.67H_2O (KOH: $x = 1.8 \cdot 10^{-4}$)

The relaxation times thus calculated are plotted in Fig. 6 as a function of reciprocal temperature. These data can be fitted well to a straight line as shown in Fig. 6. By using the Arrhenius equation

$$\tau = A \exp(\Delta H_a/RT), \quad (2)$$

the activation enthalpy ΔH_a was calculated from the slope of the straight lines to be 8.67 $kJ^{-1} \cdot mol^{-1}$. This value is quite different from those for the water reorientation in the pure hydrates (THF: 19.4 $kJ \cdot mol^{-1}$ [8], acetone: 21.2 $kJ \cdot mol^{-1}$ [9], EO: 19.7 $kJ \cdot mol^{-1}$ [6]) and ice (20–22 $kJ \cdot mol^{-1}$ [10]) and rather similar to that of the KOH-doped THF hydrate (7.4 $kJ \cdot mol^{-1}$) derived from the dielectric relaxation times [16]. It is concluded that the activation processes for the water reorientation of clathrate hydrates and ice are strongly affected by KOH dopant but is almost independent of the guest molecule and the topology of the hydrogen-bond network.

The relaxation process with the distribution of the relaxation times is described phenomenologically by Kohlrausch-Williams-Watts (KWW) function [26, 27]. In the case of the enthalpy relaxation studied by an adiabatic

calorimeter, the enthalpy relaxation rate is eventually proportional to the spontaneous temperature drift rate because of the constancy of the heat capacity within a small temperature change (ca. 0.7 K) induced by the enthalpy relaxation. The KWW function is therefore modified to

$$T(t) = A + Bt - C\exp\left[-(t/\tau)^{\beta}\right], \tag{3}$$

where $T(t)$ is the temperature at time t, $(A - C)$ the initial temperature, B the constant drift rate due to residual heat leak, C the amplitude of the relaxation, τ the relaxation time, and β the non-exponentiality parameter. For β=1, the KWW function is reduced to be the same as that derived by integrating Eq. (1). From the interpretation by Lindsey and Patterson [28], β is the extent of distribution of the relaxation times; the smaller β is, the broader the distribution becomes.

The enthalpy relaxation was observed by the two different ways: cooling (2–3 K·min^{-1}) from about 75 K down to temperatures around T_g (exothermic drift) or heating (0.02 –0.03 K·min^{-1}) up to temperatures around T_g after annealing around 56 K to obtain equilibrium states (endothermic drift). Figure 7 shows a typical exothermic temperature drift observed around 53 K and the calculated curve fitted to Eq. (3). Values of β obtained by the fitting are tabulated as follows:

T/K	50	53	56	(58)	59	(60)	61	(62)
β	0.49	0.47	0.40	0.49	0.40	0.42	0.41	0.53

The temperatures in the parentheses denote that β was obtained from the endothermic temperature drift. It was found that the β value is independent of temperature and experimental mode (exothermic or endothermic process). The average value of β (0.45) is definitely smaller than the values obtained for the pure str. II hydrates (THF: 0.70 [8], acetone: 0.67 [9]) and almost the same as the value obtained for the pure str. I EO hydrate (0.45 [6]). This is very interesting because TMO hydrate is quite different from EO hydrate though the host structure is the same; i.e., EO molecules are accommodated in both tetrakaidecahedral and dodecahedral cages (the composition of the EO hydrate is EO·6.86H_2O), and they are disordered in molecular orientation. It was concluded that the distribution of the relaxation times for the water reorientational motion depends only on the structure of the host lattice, irrespectively of the guest molecule, its orientational state, occupancy, and KOH doping.

Phase transition of str. II hydrate

During the course of the heat capacity measurement of the str. II TMO hydrate cooled continuously down to 15 K at the rate of about 0.3 K·min^{-1}, an exothermic

effect was observed around 30 K and then an endothermic one at 34.5 K. The former was due to irreversible transition from the metastable (undercooled) high

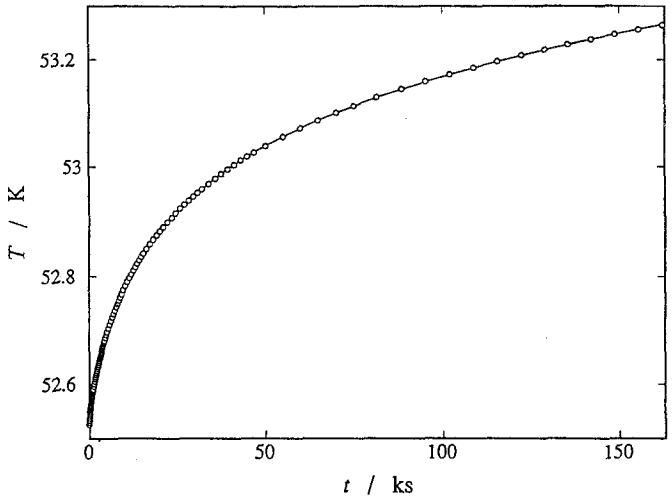

Fig. 7 Spontaneous temperature drift observed around the glass transition of TMO·7.67H_2O (KOH: $x = 1.8 \cdot 10^{-4}$)

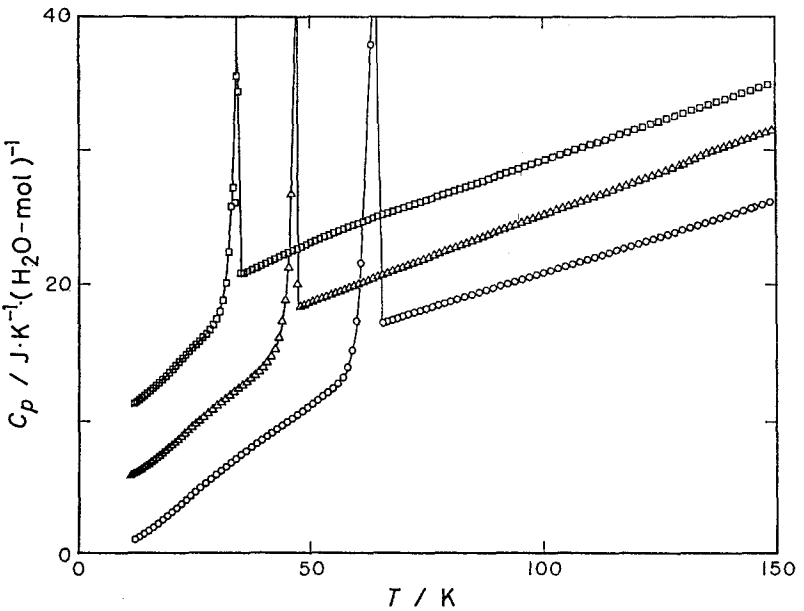

Fig. 8 Heat capacities of str. II clathrate hydrates doped with (KOH: $x = 1.8 \cdot 10^{-4}$) around the first order transitions. O : THF·17H_2O, Δ : acetone·17H_2O, □ : TMO·17H_2O. Each curve has been shifted upwards by 5 J·K^{-1}(H_2O-mol^{-1} for the sake of clarity

temperature phase to the stable low temperature one and the latter due to the corresponding reversible first-order transition. In order to complete the transformation into the low temperature phase, the sample was annealed successively at 33.6 K for 44 h, 33.1 K for 21 h, 32.1 K for 84 h, 30.5 K for 90 h, 29.5 K for 24 h, and 28.0 K for 24 h. The heat capacities plotted in Fig. 1 was for the sample thus stabilized. The heat capacities of TMO str. II hydrate is reproduced in Fig. 8 together with those of str. II THF and acetone hydrates [14, 15]. For the purpose of clarity, the heat capacities of TMO and acetone hydrates are shifted upwards by 10 $J \cdot K^{-1}(H_2O\text{-mol})^{-1}$ and 5 $J \cdot K^{-1}(H_2O\text{-mol})^{-1}$, respectively. The transition temperature of TMO hydrate (34.5 K) was lower than those of acetone (46.6 K) and THF (61.9 K) hydrates while the shape of excess heat capacity was similar to those of acetone and THF hydrates; i.e., a first order transition rising steeply on the low temperature side and exhibiting long tail on the high temperature one.

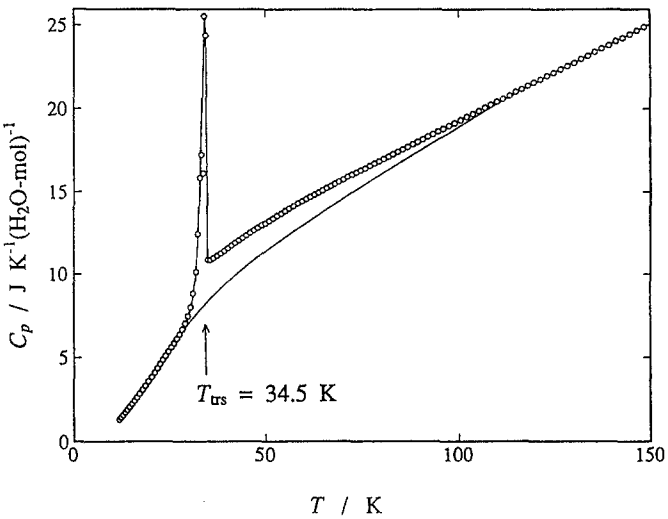

Fig. 9 Heat capacity of TMO·17H_2O (KOH: $x = 1.8 \cdot 10^{-4}$) around the phase transition. The curve shows the normal heat capacity (baseline)

To obtain the transition entropy of the TMO hydrate, the baseline was determined by fitting the heat capacity data below 27 K and above 120 K to a third-order power polynominal function. The higher limit 120 K is fairly arbitrary but adopted as the same temperature chosen in the case of acetone and THF hydrates with the aim of comparison. Figure 9 shows the baseline thus determined. The temperature dependence of the transition entropy is shown in Fig. 10 together with those of acetone and THF hydrates. The saturated value of the transition entropy is 2.36 $J \cdot K^{-1}(H_2O\text{-mol})^{-1}$, which is about 5% smaller than the transition

entropies of acetone and THF hydrates. It is noteworthy that the hydrate exhibiting lower transition temperature has smaller first-order component of the transition entropy and acquires the remaining entropy at the high temperature side of the transition.

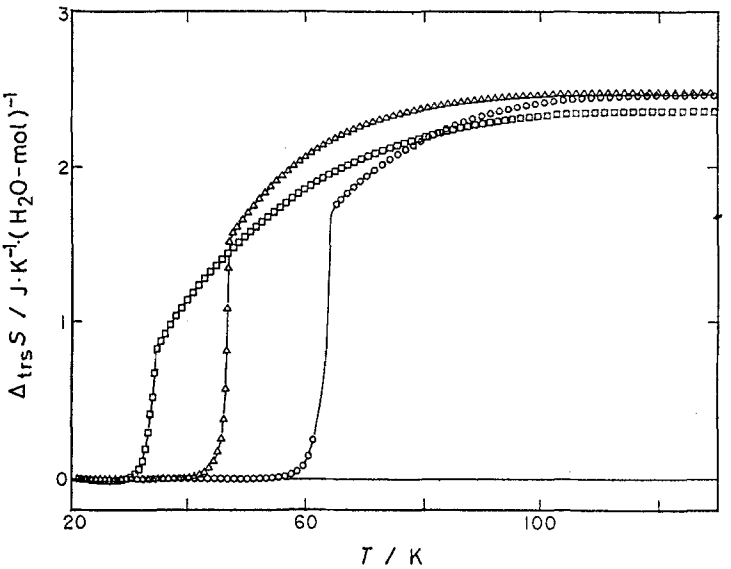

Fig. 10 Transition entropies of str. II clathrate hydrates doped with (KOH: $x = 1.8 \cdot 10^{-4}$). O : THF·17H_2O, Δ : acetone·17H_2O, □ : TMO·17H_2O

Figure 11 shows the relation between the transition temperature and the van der Waals diameter (upper) and dipole moment (lower) of the guest molecules. From the dielectric study of THF hydrate [16], it is known that both water and THF molecules become ordered at the transition temperature. Both of acetone and TMO hydrates are expected to have the same mechanism of the transition as THF hydrate because they have similar shape of excess heat capacity and entropy of the transition to those of THF hydrate. Then, it is strange that the relations given in Fig. 11 are not monotonous. Especially, it is interesting that the dipole moment of the guest molecule does not affect much on the transition temperature. Water molecule has large dipole moment (1.94 *D*) and guest-water dipole interaction should be important both in the low and high temperature phases. Other interactions, for example possible hydrogen bond formation between oxygen atom of guest molecule and host water molecule, might be important for the stability of the low and high temperature phases. Dielectric studies of acetone and TMO hydrates are required to confirme that both of the guest and water molecules are ordered in the low temperature phases. It is probable that TMO molecules are still

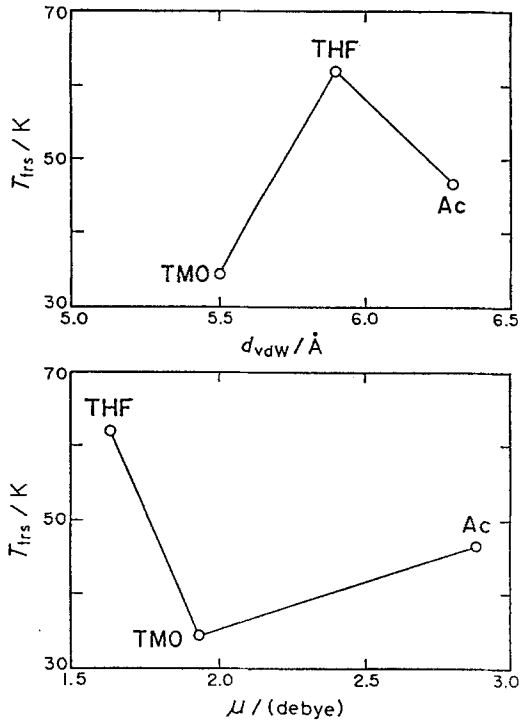

Fig. 11 Relations between the transition temperatures of str. II clathrate hydrates and the van der Waals diameters (upper) and the dipole moments (lower) of the guest molecules

disordered even in the low temperature phase. This conjecture is deduced from the fact that the heat capacity of the str. II TMO hydrate is larger than that of the str. I TMO hydrate, in spite of the fact that the guest occupancy of the str. II hydrate is smaller than that of the str. I hydrate (Fig. 1). Neutron diffraction study is also desired to determine the structure of the low temperature phase.

* * *

The authors would like to express their sincere thanks to the Nissan Science Foundation for their financial support.

References

1 D. W. Davidson, in 'Water – A Comprehensive Treatise', Ed. F. Franks, Plenum Press, New York 1973, Vol. 2, Chap. 3.
2 G. A. Jeffrey, in 'Inclusion Compounds', Ed. J. L. Atwood, J. E. D. Davies and D. D. MacNicol, Academic Press, London 1984, Vol. 1, Chap. 5.

3 D. W. Davidson and J. A. Ripmeester, in 'Inclusion Compounds', Ed. J. L. Atwood, J. E. D. Davies and D. D. MacNicol, Academic Press, London 1984, Vol. 3, Chap. 3.
4 E. Berecz and M. Balla-Achs, 'Gas Hydrates, Studies in Inorganic Chemistry 4', Elsevier, Amsterdam-Oxford-New York 1983.
5 O. Yamamuro and H. Suga, J. Thermal Anal., 35 (1989) 2025.
6 O. Yamamuro, M. Oguni, Y. P. Handa and H. Suga, J. Incl. Phenom., 8 (1990) 45.
7 Y. P. Handa, Can J. Chem., 63 (1985) 68.
8 O. Yamamuro, M. Oguni, T. Matsuo and H. Suga, J. Phys. Chem. Solids, 49 (1988) 425.
9 N. Kuratomi, O. Yamamuro, T. Matsuo and H. Suga, J. Chem. Thermodyn., 23 (1991) 485.
10 O. Haida, T. Matsuo, H. Suga and S. Seki, J Chem. Thermodyn., 6 (1974) 815.
11 O. Yamamuro, M. Oguni, T. Matsuo and H. Suga, J. Phys. Chem. Solids, 48 (1987) 935.
12 S. R. Gough, S. K. Garg and D. W. Davidson, Chem. Phys., 3 (1974) 239.
13 D. W. Davidson, Can. J. Chem., 49 (1971) 1224.
14 O. Yamamuro, M. Oguni, T. Matsuo and H. Suga, Solid State Commun., 62 (1987) 289.
15 O. Yamamuro, N. Kuratomi, T. Matsuo and H. Suga, Solid State Commun., 73 (1990) 317.
16 O. Yamamuro, T. Matsuo and H. Suga, J. Incl. Phenom., 8 (1990) 33.
17 O. Yamamuro, M. Oguni, T. Matsuo and H. Suga, J. Incl. Phenom., 6 (1988) 307.
18 Y. Tajima, T. Matsuo and H. Suga, Nature, 299 (1982) 810.
19 Y. Tajima, T. Matsuo and H. Suga, J. Phys. Chem. Solids, 45 (1984) 1135.
20 K. Moriya, T. Matsuo and H. Suga, J. Chem. Thermodyn., 14 (1982) 1143.
21 J. C. Rosso and L. Carbonnel, Compt. Rend. Acad. Sci. Paris, 274C (1972) 1108.
22 N. Kuratomi, O. Yamamuro, T. Matsuo and H. Suga, to be published.
23 F. Hollander and G. A. Jeffrey, J. Chem. Phys., 66 (1977) 4699.
24 H. Suga and S. Seki, J. Non-Cryst. Solids, 16 (1974) 171.
25 H. Suga, J. Chim. Phys. Phys-Chim. Biol., 82 (1985) 275.
26 R. Kohlrausch, Ann. Phys. (Leipzig), 12 (1847) 393.
27 G. Williams and D. C. Watts, Trans. Faraday Soc., 66 (1970) 80.
28 C. P. Lindsey and G. D. Patterson, J. Chem. Phys., 73 (1980) 3348.

Zusammenfassung — Mittels eines adiabatischen Kalorimeters wurden im Temperaturbereich 11-300 K die Wärmekapazitäten der Trimethylenoxid(TMO)klathrathydrate I und II mit Spuren an Kaliumhydroxid (x=1,810^{-4}) gemessen. Im Hydrat der Struktur I (TMO7,67H_2O) wurden bei 60 K und bei 107,9 K ein Glasumwandlungspunkt und eine Phasenumwandlung höherer Ordnung beobachtet. Die Glasumwandlung gehörte zum Einfrieren der Reorientierung der Gast-Wassermoleküle, die bei der reinen Probe bei einer Temperatur von etwa 85 K eintrat und durch den Beschleunigungseffekt von KOH verlangsamt wurde. Die Relaxationszeit der Wasserreorientierung und ihr Beitrag wurde geschätzt und mit den entsprechenden Werten anderer Klathrathydrate verglichen. Die Phasenumwandlung ist der Orientierungsordnung der Gast-TMO-Moleküle zuzuschreiben, die in den von den Wassermolekülen gebildeten Käfigen Platz nehmen. Diese Umwandlung ist höherer Ordnung und besitzt eine Umwandlungsentropie von 1,88 J·K^{-1} (TMO-mol^{-1}), was zeigt, daß mindestens 75 % der Orientierungsunordnung in der niedrigeren Tempe-raturphase erhalten bleibt. Bei dem Hydrat der Struktur II (TMO·17H_2O) trat nur eine Phasenumwandlung erster Ordnung auf: bei 34,5 K. Diese Umwandlung wird mit der Orientierungsordnung der Wassermoleküle wie im Falle des mit KOH versetzten Acetones und Tetrahydrofuranes (THF) in Verbindung gebracht. Die Umwandlungsentropie betrug 2,36 J·K^{-1} (H_2O-mol)$^{-1}$, ganz ähnlich wie bei den Aceton- und THF-Hydraten. Weiterhin wird der Zusammenhang von Umwandlungstemperatur und Entropie sowie der Gastmolekül-eigenschaften (Größe und Dipolmoment) diskutiert.